Response to the reviewers on manuscript tc-2016-144 - "Dynamic influence of pinning points on marine ice-sheet stability: a numerical study in Dronning Maud Land, East Antarctica" by L. Favier et al.

September 23, 2016

Lionel Favier, lionel.favier@ulb.ac.be

Response to Rob Arthern, Referee 1

This study describes glaciological simulations of a region of coastal East Antarctica. The simulations are performed using the BISICLES ice sheet model that has previously been shown to resolve stresses and velocities accurately at the grounding line when run at sufficiently high resolution. A novel feature of this study is the investigation of several different melt rate parameterisations and an investigation into the consequences of pinning points where detailed local surveys show that the ice is grounded, but the available continental scale bathymetric charts would suggest otherwise. The paper is logically organised and clearly written. The sensitivity studies performed make sense, the figures are appropriate and the conclusions are important enough to be published in The Cryosphere.
We thank Robert Arthern for this very positive comment.

My main concern with this paper is that I think more needs to be done to demonstrate that the results converge under grid refinement. The effect of grid resolution might be especially important if basal melting makes a sudden jump across the grounding line from a finite value to zero, or if the basal melt depends sensitively on ice draft that varies rapidly near the grounding line. Both of these conditions are relevant here and the melt parameterisations are different from those used previously, so I don't think it is enough to rely on previous investigations with this model to assess the sensitivity to grid refinement.
You are right in your analysis. We therefore performed a sensitivity analysis on a grid resolution between 250 m and 4000 m at the grounding line. In terms of contribution to sea level rise, the 250 m and 500 m resolution give close results, while the 500 and 1000 m resolution are further away. We thus chose to present the 500 m resolution in the paper, and show the sensitivity results in new supplementary material (Supplementary Figure 2) showing sea level contribution and grounding line migration.

Major considerations

There are at least three motivations for investigating the sensitivity to grid resolution more thoroughly than is done here. 1 km resolution at the grounding line seems quite coarse unless a sub-grid scheme is used to parameterise basal drag and driving stress at the grounding line. Was a sub-grid parameterisation used? Are the results sensitive to the mesh refinement?

Another important consideration is that both melt rate parameterisations have the potential to apply non-zero melt rate directly at the grounding line, with a sudden transition to no melt for grounded ice. This might impose a discontinuity in the gradient of ice thickness at the grounding line. Again, it would be good to see evidence that the model can resolve this adequately.

Also, both parameterisations depend on ice draft. Basal slopes at the grounding line can be steep. Again, this means the authors should show that their results do not depend sensitively on the grid refinement used.
No sub-grid parameterisation was used. See the previous comment for the sensitivity to resolution at the

grounding line.

I think a simulation should be included with a modified parametrization for which the melt rate goes to zero at the grounding line (perhaps by setting G=0 in Equation 1). This would reveal whether the retreat is driven mostly by melting directly at the grounding line, or by reductions in buttressing induced by melting elsewhere. We use a parameterization of sub-ice shelf melt rates according to what is generally found in the literature, based on observations and/or ocean modelling. While the experiment with zero melt at the grounding line seems at first glance interesting, its parameterization is less straightforward in combination with established parameterizations. It would furthermore require a much larger sensitivity study on the melt rates to enable meaningful conclusions. Moreover, even though we can obtain the same amount of melting at the drainage basin scale for the two melting and no-melting at the grounding line equivalent scenarios, there may be two different evolutions for the ice draft, which would differentiate the two melting over time and complexify the interpretation. Actually, the best solution would be to use an ocean model to produce melt rates (we mention it now in the text and refer to the recent publication of De Rydt and Gudmundsson (2016)). However, those two solutions (ocean modelling and more parameterization) are clearly out of the scope of our paper. Given that such inclusion would change the scope of the paper considerably, we refrained from doing so.
However, to answer the second Reviewer about the effect of the different melt rates types, we decided to run a simulation for which we switch off the sub ice shelf melting once the grounding line has started to retreat over the retrograde slope area of the Hansen glacier (melting is not altered beneath the other ice shelves). The results are now in a new supplementary figure which shows that the grounding line keeps retreating, even though not as fast as with melting. This somehow partially answers your question.

Minor corrections

P1 - Line 22. This section includes the following statement A prior retreat of the grounding line (e.g. ocean driven) resting on such an upsloping bed thickens the ice at the grounding line, which increases the ice flux and induces further retreat, etc., until a downsloping bed is reached. This description is misleading. The retreat needn't stop when a downsloping bed is reached. In the simulations of Schoof (2007) the grounding line doesn't stop at the deepest point, which is where a downsloping bed is first encountered. There is the possibility for a stable equilibrium to exist on downsloping beds, but only if upstream snowfall balances local flux at the grounding line. There is no reason for this condition to apply just because the grounding line has reached a downsloping bed. Rather, the grounding line will continue to retreat until (i) upstream snowfall balances local flux at the grounding line AND (ii) the bed is downsloping. Some glaciologists seem to think that grounding line retreat will necessarily stop when a downsloping bed is reached, modellers shouldn't be adding to this confusion.
The reviewer is right, the sentence has been rewritten as advised.

P2 – Line 25. Make clear compression/extension is in flow direction.
Done.

P5 – Explain more clearly which domain is bounded by the dotted line.
Done.

P5 – Eqn 1. I don't think G and A are melt rates. What values were used for these parameters?
The reviewer is right on the fact that they are not melt rates. Also a mistake was made when writing the equations: the actual form is $M_{b1} = H^{\alpha}(pG + (1-p)A)$ (The G parameter was changed so the equation looks like previous references to it in BISICLES related papers). The p parameter equals 1 at the grounding line and decreases exponentially away from it, as described in Cornford et al. (2015), and to which we refer to in the paper.

P6 – How does p vary? Give more details of exponential decay rate.
p equals 1 at the grounding line and decreases exponentially as a distance to the grounding line to equal 0 away from it. We now refer to Cornford et al. (2015), Appendix B2, where the way p is computed is detailed.

P7 - Line 3. It needs to be clearer which equations are being solved. The text is currently ambiguous and leaves open three different possibilities. Is it (a) the L1L2 system described by Hindmarsh (2004), (b) the L1L2 system described by Schoof and Hindmarsh (2010) or (c) the SSA* system described by Cornford et al. (2015). If the equations are the SSA* approach described by Cornford et al (2015) then these are not the same as the model described by Schoof and Hindmarsh (2010) and shouldn't be referred to as such.
The reviewer is right. The BISICLES model solves the SSA* approach described by Cornford et al. (2015). We clarified it in the text.

P7 - Eqn 5. Is any regularisation used in the sliding law for low velocities?
Yes. The results come from Berger et al 2016. Since this relates to a similar location, we simply re-used the C and Phi fields. This was not clear in the text and it's been clarified.

P8 – Imposing a trial and error value of basal freezing to prevent grounding line motion during relaxation seems slightly imprecise. An alternative approach is to fix the thickness of floating ice shelf to prevent grounding line migration during relaxation (see Arthern et al. 2015, DOI: 10.1002/2014JF003239). This approach can also incorporate dhdt observations on the grounded ice so the grounding line retreats at the observed rate during the forward simulation. It would be worth pointing out that alternative approaches to constraining the grounding line during surface relaxation are available.
Done.

P16 – Line 9. Capitalise Weertman.
Done.

Table 1. Check the units for heat capacity.
It was indeed wrong. We changed the units. We also corrected a typo in the value of γ_t.

Table 1. The parameter $\alpha 2$ is described as a tuning parameter for Mb2 not Mb1.
Right, changed.

Response to Anonymous Referee 2

1 General statement

The manuscript "Dynamic influence of pinning points on marine ice-sheets stability: a numerical study of Dronning Maud Land, East Antarctica" studies the impact of the presence of pinning points on outlet glaciers stability and their contribution to sea level rise. It shows that pinning points provide additional buttressing and therefore decrease the ice discharge by about 10%, but also that their presence strongly affects the ice shelf rheology inferred from data assimilation and therefore the model initial conditions. The authors suggest that including or omitting these pinning points impacts grounding line retreat and collapse of promontory on the timescale of several hundreds of years.
The manuscript is well written and the figures appropriate. The main point missing in the paper is that the authors do not show that their results are not resolution dependent. This can be easily done by rerunning a couple experiments with a higher mesh resolution and must be done in order to be confident that the results presented in this paper are robust.
The reviewer is perfectly right to ask for such a sensitivity study. This was also a major point raised by Robert Arthern, the other reviewer. Please look at the corresponding response above.

The interpretation of the impact of the melting is also quite ambiguous, as it differs in the discussion and conclusions. The section below describes in more details these two points and a few other specific comments.
See the responses to comments below.

2 Specific comments

p.1 l.16: "collapse" does not seem to be an appropriate word to describe a rather natural phenomenon that happens during simple grounding line retreat. This is also quite different from what is presented in the results.
The word "collapse" was indeed too strong. We now use "transition" instead.

p.2 l.11: The statement of ice rises not being detected by satellite observations is surprising: measurements of velocity and grounding line have a resolution of a few hundred meters while observations from altimetry also have an along track resolution a few hundred meters and the tracks are spaced by a few kilometers. Only bedrock topography does not have the required resolution, but sounding radars are operated in airborne and not satellite. So satellite observations, and in particular grounding line mapping should have the capability to resolve small ice rises and pinning points.
The reviewer is mostly correct and we modified the sentence accordingly.

p.2 l.34: The L-curve analysis is described in more details in Jay-Allemand et al. (2011) and not Gillet-Chaulet et al. (2012).
Agreed, we now refer to Jay-Allemand et al. (2011) instead of Gillet-Chaulet et al. (2012).

p.3 l.13: The eastern ice shelf of Thwaites Glacier experienced a complex behavior during the past coupled decades, with successive periods of acceleration and deceleration (Mouginot et al., 2014) that are not coherent with the gradual grounding line retreat and unpinning of the eastern shelf ice rise (Rignot et al., 2014). Entrainment of the Eastern ice shelf by the main ice shelf and changes in the region between the two parts of the ice shelf in this zone of intense shear is the preferred scenario to explain the complex changes observed and not a simple acceleration of this ice shelf (Mouginot et al., 2014).
The reviewer is right but what he mentions is actually related to what happened to the ice shelf before 2008. According to Mouginot et al. (2014): "After 2008, the TEIS accelerated again, but a restoration of the coupling between the two ice shelves seems unlikely as the main ice tongue calved in 2010. The recent acceleration might be better explained by a reduced buttressing of the pinning point at its terminus [Tinto and Bell, 2011; MacGregor et al., 2012] and/or the retreat of its grounding line due to enhanced thinning caused by warmer ocean water". We however rephrased, mentioning the eastern ice shelf only and not the whole ice shelf of Thwaites Glacier, to make the text clearer.

p.4 l.25-30: How sensitive are the results to these two additional excavations?
The excavation was made to avoid spurious re-advances of the grounding line that should not happen, and because the bed elevation beneath ice shelves was crudely interpolated by previous studies. For most low and several medium melting scenarios, the grounding line re-advance in the shallower water area upstream of Derwael Ice Rise. Using the original Bedmap2 bed elevation there would produce even larger re-advance, decreasing the sea level contribution for spurious reasons (which is written in the text). When the grounding line is stable or retreats, there is no sensitivity to excavations of course.

p.7 l.7: Why limit the resolution to 1km? BISICLES does not have problems using improved resolution and the domain simulated is small enough that increasing the resolution to 500 or 250 m should not too much or a problem. This is especially surprising at this manuscript focuses on the impact of small ice rises and pinning points. Authors would need to show that their results are not resolution dependent by performing a couple of the simulations that experience large changes with a grid resolution divided by two (500 m or less at the grounding line).
Done. See my answer to the first reviewer above.

p.7 l.16: How are the inversions of C and φ performed? Are they done simultaneously or one after the other? Are they done over the same region of different parts of the domain? This is not clear form the text and is an important question as changes in friction and stiffening factor can have a similar impact on ice flow.
The two inversions are performed simultaneously and over the whole domain, which we added in the text.

p.8. l.10: How large is the melt rate in this region? It is surprising to see that adding just 1 m/yr drastically change the grounding line evolution from rapid retreat to small advance. This suggests that the model is very sensitive to this parameter.
More precisely, the drainage basin of Hansenbreen in particular is very sensitive to this parameter, which is because the retrograde bed slope area (towards the ocean) starts few kilometres upstream of the current grounding line. To answer your question, we had a personal communication with Dr Depoorter (Depoorter et al., 2013) who recalculated the melting for the basins that we simulated. The sub-ice shelf melting undergone by the Hansenbreen glacier is about 3.5 Gt/yr. In the analogous study of Rignot et al. (2013), the overall sub-ice shelf melting is 7 Gt/yr but takes into account the two neighbouring glaciers to the west (called Borchgrevink in his paper). Our low, medium and high melt scenarios give more or less 2, 3.5 and 5 Gt/yr, respectively, after initialisation.

p.12 l.17-18: This statement contradicts what is shown on Fig.7. The type of melt rate applied seems to play a significant role in at least the rate of grounding line retreat as the three upper plots with melting type Mb1 all have a similar grounding line evolution, while the three lower ones with melting type Mb2 also have a similar behavior, distinct from the previous one. And this is actually quite different from what is summarized in the conclusions.
Yes, the two melt rates affect differently the buttressing from the ice shelf. We agree that the amount of retreat that can be attributed to MISI is difficult to assess. We therefore decided to add a Sup figure, comparable to Figure 6(b) for which we swith off the sub-ice shelf melting beneath the Hansen glacier once the grounding line enters the retrograde bed slope area. This somehow enables to evaluate the effect of MISI and sub ice-shelf melting in the retreat.

3 Technical comments

p.2 l.6: “to more investigated” → “to be more investigated”
Done.

p.2 l.32: “overmatching” → “over fitting”
Done.

p.3 l.30: Which field measurements?
Radar and GPS: we added a reference to Drews (2015).

p.4 l.2: How do the first decades of the simulations compare with the observations that we have of the past couple decades?
The surface elevation change rates after the 50 years of relaxation are shown in Figure 2. These are comparable to other studies such as Cornford et al. (2015). In terms of velocities, the results remains similar to the initial velocities that were used to infer the C and ϕ parameters. After the relaxation phase, the buttressing is modified with the new sub-ice shelf melting and significant changes start with the retreat of the Hansenbreen glacier, followed by much slower changes elsewhere.

p.4 l.3: How were these melt rates chosen? How do they compare with observations?
As said further in the text, we chose sub-ice shelf melt rates that are similar over the drainage basins to current values from Rignot et al. (2013) and Depoorter et al. (2013), with a personal communication from M. Depoorter who computed the sub-ice shelf melt rates for the specific basins of Hansenbreen and its two neighbours in the west, which were taken as one area in Rignot et al. (2013) under the name of Borchgrevink. These are for the medium melt rates scenarios. The low and high melt rates scenarios represent more or less half and twice the current values. We added a few words in the text and a Supplementary Table to summarize these numbers.

p.4 l.32: Authors should quickly summarize the model or observations that were used to derive this surface mass balance, and the year that is reproduces.
Done.
Fig. 2 caption: Notations should be consistent: B/S or Be /S
Done.

p.7 l.24-25: Not clear. Simply say that you use the improved velocity and the standard bedrock topography maps.
We clarified the text.

p.8 l.19: What are the values from Rignot et al. (2013) and Depoorter et al. (2013) and what are the values used in the simulation for the different ice shelves? A table with the melt observed and used for each ice shelf could help make this comparison.
We added a Supplementary Table to summarize current values given in Rignot et al. (2013) and given by M. Depoorter as personal communication, computed following the method given in Depoorter et al. (2013).

p.9 l.8: “mismatch” → “difference”
Done.

p.9 Fig. 3: This figure would be much clearer with colors.
Done.

p.11 Fig.5: Same as Fig.3, would be better with colors.
Done.

p.11 Fig.5 caption: “Velocity absolute” → “Absolute velocity”
Done.

p.12 l.7: There are many other very relevant references for the collapse of the WAIS.
Right, We added the following ones: Mercer (1978); Joughin and Alley (2011).

p.12 l.13: “In total” → “Overall”
Done.

p.16 l.9: Weertman, capital missing
Done.

4 References

Depoorter, M. A., J. L. Bamber, J. A. Griggs, J. T. M. Lenaerts, S. R. M. Ligtenberg, M. R. van den Broeke, and G. Moholdt, Calving fluxes and basal melt rates of Antarctic ice shelves, Nature, doi:10.1038/nature12567, 2013.

Gillet-Chaulet, F., et al., Greenland ice sheet contribution to sea-level rise from a new generation ice-sheet model, Cryosphere, doi:10.5194/tc-6-1561-2012, 2012.

Jay-Allemand, M., F. Gillet-Chaulet, O. Gagliardini, and M. Nodet, Investigating changes in basal conditions of Variegated Glacier prior to and during its 1982-1983 surge., Cryosphere, doi:10.5194/tc-5-659-2011, 2011.

Mouginot, J., E. Rignot, and B. Scheuchl, Sustained increase in ice discharge from the Amundsen Sea Embayment, West Antarctica, from 1973 to 2013, Geophys. Res. Lett., doi:10.1002/2013GL059069, 2014.

Rignot, E., S. Jacobs, J. Mouginot, and B. Scheuchl, Ice shelf melting around Antarctica, Science, doi:10.1126/science.123579
2013.

Rignot, E., J. Mouginot, M. Morlighem, H. Seroussi, and B. Scheuchl, Widespread, rapid grounding line retreat of Pine Island, Thwaites, Smith and Kohler glaciers, West Antarctica from 1992 to 2011, Geophys. Res. Lett., doi: 10.1002/2014GL060140, 2014.

References

Cornford, S. L., Martin, D. F., Payne, a. J., Ng, E. G., Le Brocq, a. M., Gladstone, R. M., Edwards, T. L., Shannon, S. R., Agosta, C., van den Broeke, M. R., Hellmer, H. H., Krinner, G., Ligtenberg, S. R. M., Timmermann, R., and Vaughan, D. G. (2015). Century-scale simulations of the response of the West Antarctic Ice Sheet to a warming climate. *The Cryosphere*, 9(2):1887–1942.

De Rydt, J. and Gudmundsson, G. H. (2016). Coupled ice shelf-ocean modeling and complex grounding line retreat from a seabed ridge. *Journal of Geophysical Research: Earth Surface*, (March).

Depoorter, M. a., Bamber, J. L., Griggs, J. a., Lenaerts, J. T. M., Ligtenberg, S. R. M., van den Broeke, M. R., and Moholdt, G. (2013). Calving fluxes and basal melt rates of Antarctic ice shelves. *Nature*, 502(7469):89–92.

Drews, R. (2015). Evolution of ice-shelf channels in Antarctic ice shelves. *The Cryosphere*, 9(3):1169–1181.

Gillet-Chaulet, F., Gagliardini, O., Seddik, H., Nodet, M., Durand, G., Ritz, C., Zwinger, T., Greve, R., and Vaughan, D. G. (2012). Greenland ice sheet contribution to sea-level rise from a new-generation ice-sheet model. *The Cryosphere*, 6(6):1561–1576.

Jay-Allemand, M., Gillet-Chaulet, F., Gagliardini, O., and Nodet, M. (2011). Investigating changes in basal conditions of Variegated Glacier prior to and during its 1982-1983 surge. *Cryosphere*, 5(2005):659–672.

Joughin, I. and Alley, R. B. (2011). Stability of the West Antarctic ice sheet in a warming world. *Nature Geoscience*, 4(8):506–513.

Mercer, J. (1978). West Antarctic ice sheet and CO2 greenhouse effect: a threat of disaster. *Nature*, 271.

Mouginot, M., Rignot, E., Gim, Y., Kirchner, D., and Lemeur, E. (2014). Low-frequency radar sounding of ice in East Antarctica and southern Greenland. *Annals of Glaciology*, 55(67):138–146.

Rignot, E., Jacobs, S., Mouginot, J., and Scheuchl, B. (2013). Ice-Shelf Melting Around Antarctica. *Science*, 341(6143):266–270.

Dynamic influence of pinning points on marine ice-sheet stability: *a numerical study in Dronning Maud Land, East Antarctica*

Lionel Favier[1], Frank Pattyn[1], Sophie Berger[1], and Reinhard Drews[1]

[1]Laboratoire de Glaciologie, DGES, Université libre de Bruxelles, Brussels, Belgium

Correspondence to: Lionel Favier (lionel.favier@ulb.ac.be)

Abstract.

The East Antarctic ice sheet is likely more stable than its West Antarctic counterpart, because its bed is largely lying above sea level. However, the ice sheet in Dronning Maud Land, East Antarctica, contains marine sectors that are in contact with the ocean through overdeepened marine basins interspersed by grounded ice promontories and ice rises, pinning and stabilising the ice shelves. In this paper, we use the ice-sheet model BISICLES to investigate the effect of sub-ice shelf melting, using a series of scenarios compliant with current values, on the ice-dynamic stability of the outlet glaciers between the Lazarev and Roi Baudouin ice shelves over the next millennium. Overall, the sub-ice shelf melting substantially impacts the sea-level contribution. Locally, we predict a short-term rapid grounding-line retreat of the overdeepened outlet glacier Hansenbreen, which further induces the ~~collapse~~transition of the bordering ice promontories into ice rises. Furthermore, our analysis demonstrates that the onset of the marine ice-sheet retreat and subsequent promontory ~~collapse~~transition into ice rise is controlled by small pinning points, mostly uncharted in pan-Antarctic datasets. Pinning points have a twofold impact on marine ice sheets. They decrease the ice discharge by buttressing effect, and play a crucial role in initialising marine ice sheets through data assimilation, leading to errors in ice-shelf rheology when omitted. ~~Our results show that unpinning has a small effect on sea-level rise but locally affects the timing of grounding-line migration, advancing the collapse of a promontory by hundreds of years. On the other hand, omitting the same pinning point in data assimilation decreases the sea-level contribution by 10% and delays the promontory collapse by almost a millennium.~~Our results show that unpinning increases the sea level rise by 10% while omitting the same pinning point in data assimilation decreases it by 10%, but the more striking effect is in the promontory transition time, advanced by two centuries for unpinning and delayed by almost half a millennium when the pinning point is missing in data assimilation. ~~This very subtle influence of p~~Pinning points exert a subtle influence on ice dynamics ~~acts on~~at the kilometre scale~~ and~~, which calls for a better knowledge of the Antarctic margins~~ that will improve sea-level predictions~~.

1 Introduction

The marine ice-sheet instability (MISI) (Weertman, 1974; Thomas and Bentley, 1978) hypothesis states that a marine ice sheet having its grounding line - the boundary between grounded and floating ice - resting on an upsloping bed towards the sea is potentially unstable. A prior retreat of the grounding line (e.g. ocean driven) resting on such an upsloping bed thickens the ice at the grounding line, which increases the ice flux and induces further retreat, etc., until a downsloping bed is reached, provided that upstream snowfall balances local flux at the grounding line. The MISI hypothesis has been verified using the boundary layer theory developed by Schoof (2007) and simulated with numerical studies (e.g. Durand et al., 2009). Because most of the West Antarctic ice sheet (WAIS) rests on an upsloping bed, the potential retreat of its grounding line is widespread. Therefore, the vulnerability of the WAIS to current climate change has been extensively studied (e.g. Cornford et al., 2015; Deconto and Pollard, 2016). On the other hand, the East Antarctic ice sheet (EAIS) is less vulnerable to retreat on short time scales and its stability has therefore been less debated. However, a recent study investigating ice-sheet instability in Antarctica (Ritz et al., 2015) pointed out the likeliness for unstable retreat of grounding lines in Dronning Maud Land (DML), East Antarctica, over the next two centuries. ~~For those reasons and the fact that~~Moreover, the EAIS hosts ten times more ice than the WAIS and, therefore its future stability needs to be more investigated.

In ~~Dronning Maud Land~~DML, the floating margins of outlet glaciers are buttressed by numerous topographic highs, which attach to the otherwise floating ice shelves from beneath and form icy pinning points protruding through ice. Pinning points are either called ice rises or ice rumples. The former exhibit a local-flow regime while the latter are still overridden by the main ice flow. Ice promontories are ice rises that are connected to the mainland through a grounded saddle. Most ice rumples and a significant number of ice rises are smaller than 10 km^2 (Matsuoka et al., 2015)~~, and thus prone to be missed by satellite observations~~Even though they are common features in ~~Dronning Maud Land~~DML, they are often missing in the bathymetry because airborne radar data are not closely enough spaced. This issue was recently pointed out in two studies revealing a series of uncharted pinning points from ice-sheet modelling (Fürst et al., 2015) and observations (Berger et al., 2016).

The back stress induced by pinning points - even small ones, i.e., few km^2 in area - buttresses ice shelves, hampering ice discharge towards the ocean. Because simulating pinning points requires accurate treatment of grounding-line dynamics, they have only recently been considered in ice-sheet models: Goldberg et al. (2009) and Favier et al. (2012) investigated the transient effect of pinning points for idealised geometry, using ice-sheet models of varying complexity. In both studies, including a pinning point beneath an ice shelf in steady state significantly slows down the ice flow, inducing a grounding-line advance until the grounded ice sheet fully covers the pinning point. The development of an ice rise over a deglaciation and its further stability among an ice sheet/shelf system in steady state was lately simulated by Favier and Pattyn (2015), even though the stability of ice rises has been known for decades (Raymond, 1983). Favier and Pattyn (2015) also demonstrated that ice promontories are transient features collapsing into ice rises during ice-sheet deglaciation.

Both studies of Favier et al. (2012) and Favier and Pattyn (2015) used ice-sheet models of sufficient complexity to accurately quantify the stress pattern in the pinning-point's vicinity: ice is compressed along flow upstream of the pinning point, sheared when flowing around it, and stretched along flow farther downstream. The levels of extensive stress computed were higher than what can be accommodated by ice creep, which in reality leads to brittle fracturing and rifting (Humbert and Steinhage, 2011). Pinning points thus affect ice rheology by increasing local-scale deformability, which further impacts surface velocities.

Initialisation of transient simulations relies on data assimilation methods (e.g. MacAyeal, 1993). These are applied to observed ice geometry and surface velocity to infer poorly known parameters such as basal friction and ice stiffening/softening, the latter mostly accounting for crevasse-weakening and ice anisotropy. These parameters are inferred by minimising a cost function, which sums the mismatch between observed and modelled surface velocities and Tikhonov regularisation terms for each inferred parameter, the latter terms being tuned to provide continuous fields and avoid ~~overmatching~~over fitting. Even though regularisation remains subjective, a sound trade-off between reducing velocity mismatch and ~~overmatching~~over fitting can be achieved using the L-curve method (e.g. Morlighem et al., 2013; Jay-Allemand et al., 2011).

In areas where ice/bed geometry and surface velocity are not correctly resolved, the inferred parameters are likely flawed. Recently, Fürst et al. (2016) investigated the band of floating ice that can safely calve off without increasing ice discharge to the ocean. This result stems from a static analysis of the force balance between ocean pressure and ice internal stress state, which can flaw further transient simulations if pinning points are not accounted for (Fürst et al., 2015). Berger et al. (2016) demonstrated through a diagnostic study that omitting the contact between a topographic high and the ice-shelf base during data assimilation yields excessive ice-shelf stiffening, which compensates for the lack of basal friction in order to match observed surface velocities. However, it remains unclear how such erroneous initialisation impacts the transient behaviour of the ice-sheet/shelf system, which is a question we address here.

Unpinning may occur over various time scales due to progressive ice-shelf thinning (Paolo et al., 2015; Pritchard et al., 2012), erosion, rising sea level, tidal uplift (Schmeltz et al., 2001), or through the developments of rifts (Humbert and Steinhage, 2011). However, unpinning of Antarctic ice shelves has been poorly documented so far. According to Mouginot et al. (2014), the best explanation for the acceleration of the eastern ice shelf of Thwaites Glacier in the Amundsen sea sector since 2008 ~~is potentially linked to the unpinning of the ice-shelf terminus~~might be reduced buttressing from the pinning point at its terminus (also hypothesise in Tinto and Bell, 2011), even though other mechanisms such as sub-ice shelf melting may also be at play. In Larsen C ice shelf, the unpinning of the Bawden and Gipps ice rises was simulated diagnostically (i.e., without ice geometry changes) by manually decreasing the basal drag (Borstad et al., 2013), which substantially accelerated the ice flow by up to 200 m a^{-1} over an extent of about 100 km upstream. However, the transient evolution of ice geometry and velocity after unpinning has not been investigated so far. We also address this question in this paper.

The studied area is situated between the Lazarev and Roi Baudouin ice shelves in ~~Dronning Maud Land~~DML and contains a number of ice streams flowing around the Sør Rondane mountain range to the west and the Yamato mountain range to the east. The coastal belt comprises a series of ice rumples, ice rises and promontories buttressing the ice shelves. From west to east, the three outlet glaciers of Tussebreen (TB), Hansenbreen (HB) and West Ragnhild (WRG) are potentially unstable because their beds lie below sea level and dip towards the interior of the ice sheet. The grounded area is well constrained in the Antarctic-wide bed elevation datasets (Fretwell et al., 2013) as the latter incorporate airborne radio-echo sounding data collected during the Austral summer of 2010/2011 (Callens et al., 2014, 2015). TB and HB are separated by the TB/HB promontory, HB and WRG by the HB/WRG promontory. The calving front of HB is in contact with two pinning points, hereafter called PPhs, and the calving front of WRG with another pinning point, hereafter called PPw (Figure 1).

The pinning point PPw strongly buttresses the ice shelf of WRG (Berger et al., 2016). ~~However, its surface velocities are not correctly resolved (Rignot et al., 2011), and its ice/bed geometry does not appear (Fretwell et al.,2013) in the Antarctic-wide datasets. The high-resolution field of surface velocities derived by berger et al. (2016) from the ERS1/2 and ALOS-PALSAR satellites shows that PPw is virtually stagnant, which is also shown by field measurements (Drews, 2015). Berger et al. (2016) combined the high-resolution velocities with modified ice/bed geometry around PPw based on ground measurements (Drews,~~

~~2015), and employed this comprehensive dataset for model initialisation.~~However, Antarctic-wide dataset do not correctly resolve surface velocities (Rignot et al., 2011) and ice/bed geometry (Fretwell et al., 2013) in the vicinity of PPw. This has been improved by Berger et al. (2016) who modified the corresponding datasets in the surroundings of PPw with field-based data of ice thickness and velocity (Drews, 2015). The modified datasets are used here for model initialisation.

In this study, we use the adaptive-mesh ice-sheet model BISICLES to investigate: (i) the future behaviour of these outlet glaciers (see previous paragraph) with respect to potential unstabilities, (ii) their dynamic response to PPw unpinning ~~and~~, (iii) the dependency of the transient results on the model initialisation, using datasets either resolving PPw (Berger et al. (2016)'s high-resolution dataset), or not correctly resolving PPw (Rignot et al. (2011)'s velocities in combination with ice/bed geometry from Fretwell et al. (2013)), and (iv) the effect of two sliding laws and six sub-ice shelf melting parametrisations comparable to observed values. ~~Each of the first three point is addressed~~The three distinct initial conditions stemming from (ii) and (iii) are used to run ~~with~~ transient simulations ~~run~~ over the next millennium ~~with an ensemble of six different sub-ice shelf melting scenarios in combination with two types of sliding laws, because these parameters are poorly constrained by observations~~forced by the different melting parametrisations. The 36 resulting simulations give a comprehensive overview of ~~the future evolution of the ice sheet~~future ice dynamics in DML and testify to the importance of including even small pinning points in the observational datasets.

2 Datasets and Methods

2.1 Input data

Each experiment consists of an initialisation by data assimilation and a subsequent set of transient simulations. The former requires surface velocity, ice thickness, bed elevation, ~~and~~ englacial temperatures, and two initial fields for ice stiffening factor and basal friction coefficient. The latter requires ice thickness, bed elevation, initial englacial temperatures, ~~an~~two fields for ice stiffening factor and basal friction coefficient ~~field~~ (the latter two computed by the data assimilation), surface mass balance, and basal mass balance of the ice shelves.

The computational domain covers an area of about 40,000 km^2 and is illustrated in Figure 1. Two distinct datasets for flow-field and ice/bed geometry were employed. The *standard* dataset comprises surface velocities from Rignot et al. (2011) and ice/bed geometry from Fretwell et al. (2013) (the Bedmap2 dataset). The *high-resolution* dataset uses the observations of Berger et al. (2016) on the WRG ice shelf, which account for PPw in both surface velocities and ice/bed geometry (the latter called mBedmap2). These two datasets only differ for the WRG ice shelf and are otherwise identical.

Modelling grounding-line advance as a response to ocean-induced perturbation is very sensitive to sub-ice shelf bathymetry, which is roughly interpolated in our studied domain (Le Brocq et al., 2010) and thus largely uncertain. As a consequence, the water column beneath ice shelves is in places very shallow, which can cause spurious ice-shelf re-grounding. In order to make the bathymetry more coherent with both bed elevation at the grounding line and (unpublished) measurements near the ice-shelf front, we lowered the ~~bathymetry~~bed elevation beneath the ice shelves in a two-step procedure. First, we excavated a 250 m thick uniform layer 30 km away from the grounding line, ensuring a smooth connection with the grounded area with

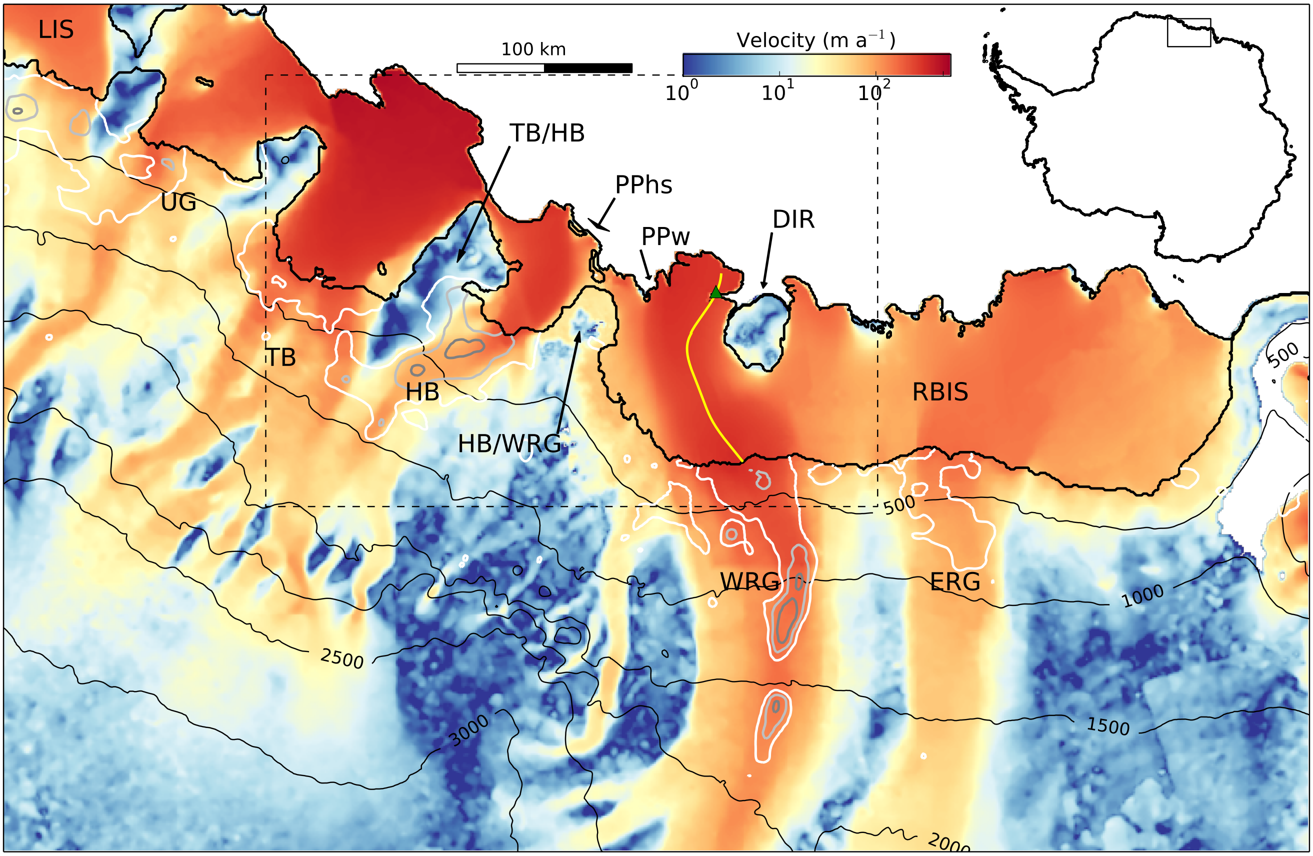

Figure 1. Computational domain with the extended flow-field from Berger et al. (2016) in the background. The thick black lines show the grounding line and the calving front. The thin black lines show ice surface elevation contours every 500 m. The white, light grey and dark grey lines are bed elevation contours of -500 m, -750 m and -1000 m, respectively. The yellow line shows the central trench of the bathymetry excavation (Section 2.1), and the green triangle the supporting bathymetric data (K. Leonard, personal communication, 2012). The dashed box shows the domain of interest shown in Figure 2 to Figure 7, and in Supplementary Figures and Movie. LIS: Lazarev Ice Shelf; UG: Unnamed Glacier; TB: Tussebreen; HB: Hansenbreen; HB/WRG: promontory in between HB and WRG; TB/HB: promontory in between TB and HB; DIR: Derwael Ice Rise; RBIS: Roi Baudouin Ice Shelf; WRG: West Ragnhild Glacier; ERG: East Ragnhild Glacier. We also name a group of two pinning points PPhs located at the front of HB, and the pinning point PPw at the front of WRG.

a 1-D Gaussian function. The second part of the excavation is based on unpublished bathymetric data collected during a 2011 oceanographic survey (K. Leonard, personal communication, 2012), which shows a more than 850 m deep trough ~~more than 850 m deep~~ cutting through the continental shelf between PPw and Derwael Ice Rise (DIR) (Figure 1). This feature may be the relict of past ice sheet erosion from the WRG ice stream when the grounding line was closer to the continental shelf break (Livingstone et al., 2012). We therefore assume the presence of a narrow trough cutting through the bathymetry beneath the ice shelf linked to the deepest section at the grounding line (yellow line in Figure 1). The second excavation was done across-flow

~~excavation uses~~using a 1-D Gaussian-shaped function (its half-width is 15 km based on the ice-stream cross-section extent). Both excavations are included in the *standard* as well as the *high-resolution* datasets.

The surface mass balance was derived by Arthern et al. (2006), who combined in-situ measurements (most of them between 1950 and 1990) and satellite observations of passive microwave (from 1982 to 1997) using a geostatistical approach, and is constant in time.

For the ice-shelf basal mass balance, we applied two melt-rate parametrisations M_{b1} and M_{b2}, based on Gong et al. (2014) and Beckmann and Goosse (2003), respectively. The former is a scheme that allows the highest melt rates to follow the grounding-line migration, using a combined function of ice thickness and distance to the grounding line, defined as

$$\cancel{M_{b1} = \alpha_1 H^{\alpha_2} (pG + (1-p)\,A)} M_{b1} = H^{\alpha} (pG + (1-p)\,A), \tag{1}$$

where H is the ice thickness, and G and A are ~~the grounding line and ambient melt rates~~tuning parameters to constrain melt rates at the grounding line, and away from the grounding line, respectively. The value of p decreases exponentially with distance to the grounding line, taking the value of 1 at the grounding line and 0 away from it (Cornford et al., 2015, Appendix B2)~~. α_1 and α_2 are tuning parameters~~, and α is a tuning parameter. The M_{b2} parametrisation is based on the difference between the freezing point of water and ocean temperature near the continental shelf break (as developed in Beckmann and Goosse, 2003). The virtual temperature T_f at which the ocean water freezes at the depth z_b below the ice shelf is defined as

$$T_f = 273.15 + 0.0939 - 0.057 S_o + 7.64 \times 10^{-4} z_b, \tag{2}$$

where S_o is the ocean salinity (set at 34.5 psu from Schmidtko et al. (2014), confirmed by K. Leonard, personal communication, 2012). The melt rates M_{b2} are prescribed as

$$M_{b2} = \frac{\rho_w c_{p_0} \gamma_T F_{melt} (T_0 - T_f)}{L_i \rho_i} \tag{3}$$

where ρ_w is the density of water, c_{p_0} the specific capacity of the ocean mixed layer, γ_T the thermal exchange velocity, T_0 the ocean temperature (set at -1.5 °C from Schmidtko et al. (2014) and K. Leonard, personal communication, 2012), L_i the latent heat capacity of ice, ρ_i the density of ice (Table 1 for the value of parameters) and F_{melt} a tuning parameter.

Ice temperature data are provided by a three-dimensional thermo-mechanical model (updated from Pattyn, 2010) and are constant in time.

2.2 Ice-sheet modelling

The simulations were performed using the finite volume ice-sheet model BISICLES (http://BISICLES.lbl.gov)~~ that solves the Schoof-Hindmarsh approximation (called L1L2 in Hindmarsh et al, 2004) of the full-Stokes equations~~. The model solves the Shallow Shelf Approximation (SSA) and includes vertical shearing in the effective strain rate (the model is fully detailed in Cornford et al. (2015)), which makes the ice softer than the traditional SSA approach at the grounding line, and induces similar ice sheet behaviour compared to full-Stokes models (Pattyn and Durand, 2013) when using of sub-kilometric resolution at the grounding line. We assessed the sensitivity to the grid resolution at the grounding line, between 250 m and 4000 m, of ice sheet

Table 1. Model parameters

Parameter	Symbol	Value	Unit
Ice density	ρ_i	917	kg m^{-3}
Water density	$\cancel{\rho_i}\rho_w$	1028	kg m^{-3}
Gravitational acceleration	g	9.81	m s^{-2}
Glen's exponent	n	3	
Basal friction exponent	m	(1, 1/3)	
Grid resolution		4000 down to 500	m
Specific heat capacity of ocean mixed layer	c_{p_0}	3974	J kg^{-1} K^{-1}
Thermal exchange velocity	γ_T	$\cancel{10^{-1}}10^{-4}$	m s^{-1}
Temperature of the ocean	T_0	271.65 (-1.5 °C)	K
Salinity of the ocean	S_O	34.5	psu
Latent heat capacity of ice	L_i	3.35 10^5	J kg^{-1}
Tuning parameter for $\cancel{M_{b2}}M_{b1}$	$\cancel{\alpha_2}\alpha$	3	
Tuning parameter for M_{b1}	$\cancel{\alpha_1}$G	(25, 50, 100) 10^{-9}	
Tuning parameter for M_{b1}	A	0	
Tuning parameter for M_{b2}	F_{melt}	(0.01, 0.02, 0.03)	

changes (Supplementary Figure 2). The contribution to sea level change and grounding-line migration converge below 500 m. We thus used 500 m resolution at the grounding line for all the transient simulations, up to 4000 m farther inland (Table 2.1). The equations are solved on an adaptive horizontal 2-D grid rendered by the Chombo framework. ~~The L1L2 solution improves the Shallow Shelf Approximation by adding a vertical shearing stress component - based on the Shallow Ice Approximation - to the effective strain rate (the model is fully detailed in Cornford et, 2015).~~ Data assimilation is performed by a control method that solves the adjoint system of equations, as described in Appendix B1 of Cornford et al. (2015). ~~During transient simulations, we applied one kilometre resolution at the grounding line (Table 2.1)~~. The relationship between stresses and strain rates is given by the Glen's flow law:

$$\boldsymbol{S} = 2\phi\eta\dot{\boldsymbol{\varepsilon}}, \tag{4}$$

where $\boldsymbol{S}$ is the deviatoric stress tensor, $\dot{\boldsymbol{\varepsilon}}$ is the strain rate tensor, η is the effective viscosity (depending on ice temperatures and effective strain rate), and ϕ is a stiffening factor representing non-thermal viscosity effects, such as crevasse-weakening and ice anisotropy. The basal friction between the grounded ice sheet and the bed is governed by a Weertman-type sliding law (Weertman, 1957):

$$\boldsymbol{\tau}_b = \begin{cases} -C|\boldsymbol{u}_b|^{m-1}\boldsymbol{u}_b & \text{if} \quad \dfrac{\rho_i}{\rho_w}H > -b \\ 0 & \quad\quad \text{otherwise} \end{cases} \tag{5}$$

s where $\boldsymbol{\tau}_b$ is the basal traction, C is the friction coefficient, m is the friction exponent and $\boldsymbol{u}_b$ is the basal velocity. Initial fields of C and ϕ were both inferred (simultaneously and over the computational domain) with the control method applied to ice/bed geometry and surface velocities, using the same procedure as described in Berger et al. (2016), as well as the results obtained for the C and ϕ fields.

2.3 Description of the experiments

Initialisation

Three sets of initialisations with both linear ($m = 1$) and nonlinear ($m = 1/3$) sliding were performed for C, ϕ (both inferred with the control method), and the initial ice/bed geometry:

- B_e/S: The control method and the transient simulations use the *high-resolution* dataset ~~, so that~~(PPw is ~~used for~~included in model initialisation and evolution).
- B_e/U: This is a variant of B_e/S in which transient simulations start from bed elevation and ice thickness without resolving PPw - we use Bedmap2 instead of mBedmap2 - in order to simulate unpinning.
- RF/S: The control method and the transient simulations use the *standard* dataset ~~, hence excluding~~(PPw ~~for~~is excluded from ~~both~~ initialisation and evolution).

Because there is no friction beneath ice shelves, we set the value of the friction coefficient C in case of further ice-shelf regrounding during transient simulations at 500 Pa m^{-1} a. This number causes high basal sliding (comparable to sliding beneath ice streams), which reflects the idea of a sediment-filled bathymetry, and is motivated by the sediment layer ~~observed~~inferred from airborne radar and ice-sheet modelling upstream of the WRG grounding line (Callens et al., 2014).

After model initialisation, the ice-sheet geometry was relaxed for 50 years prior to the transient simulations, in order to decrease the ice-flux divergence due to artefacts of interpolation and other sources of geometry errors (such as in Cornford et al., 2015). During the relaxation, we used mass conservation to compute melt rates beneath ice shelves (assuming steady state), which gives values in line with current observations (Depoorter et al., 2013; Rignot et al., 2013). However, applying such melt rates beneath the HB ice shelf leads to a rapid retreat of the grounding line during the time span of the relaxation. We solved this issue by applying a positive basal mass balance (i.e., accretion) of 1 m a^{-1} during the relaxation, which helps to stabilise the ice shelf, but leads to few kilometres advance of the grounding line (Stabilising the ice sheet during relaxation can also be done by fixing the ice shelf thickness, such as in Arthern et al. (2015)). Surface elevation change rates (and their spatial gradients) drop by an order of magnitude (Figure 2) during relaxation.

Transient scenarios

Each initialisation is followed by 12 different transient simulations, applying either linear or nonlinear sliding together with 6 different prescribed sub-ice shelf melt rates, M_{b1} and M_{b2}, each with 3 different amplitudes - low, medium and high - set

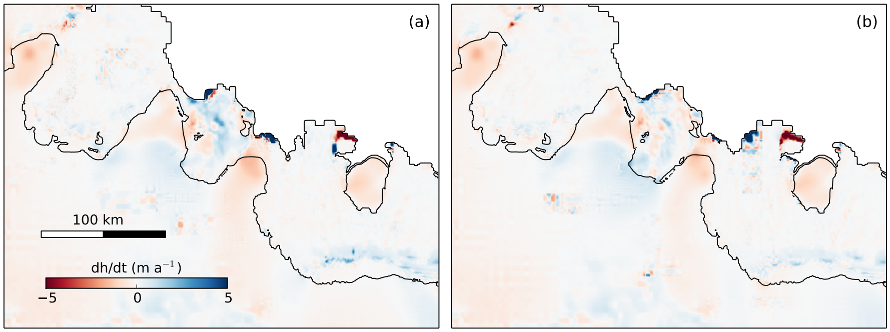

Figure 2. Surface elevation change rates ~~within the region of interest~~ after relaxation of ~~B/S~~Be/S and ~~B/U~~Be/U (a) and RF/S (b) initialisations, for linear sliding.

Table 2. Setup of all 36 experiments. The name of each experiment reflects the dataset used for initialisation, its initial ice/bed geometry, the form of sliding law, and the type and amplitude of the melt-rates.

Experiment name	Dataset for		m	Melt rates	
	Data assimilation	Initial geometry		Type	Amplitude
$B_e/S/L/M_{bi}/A_j$	*high-resolution*	*high-resolution*	1	i=(1,2) for M_{b1} or M_{b2}	j=(l,m,h) for (low, medium, high)
$B_e/S/NL/M_{bi}/A_j$			1/3		
$B_e/U/L/M_{bi}/A_j$	*high-resolution*	*standard*	1		
$B_e/U/NL/M_{bi}/A_j$			1/3		
$RF/S/L/M_{bi}/A_j$	*standard*	*standard*	1		
$RF/S/NL/M_{bi}/A_j$			1/3		

by tuning the parameters α, G and A for M_{b1}, and F_{melt} for M_{b2} (Table 1). The naming convention adopted for transient simulations and the corresponding parameters are given in Table 2.

The sum of initial medium melt rates over the ice shelves yields values that are comparable to current values (Rignot et al., 2013; Depoorter et al., 2013, and M. Depoorter, personal communication, 2016; Supplementary Table). The sum of low and high melt rates represent approximately half and twice the sum of medium melt rates, respectively. Initial melt rates M_{b1} and M_{b2} of medium amplitude are shown in Figure 3 for the B_e/S initialisation. For similar amplitudes, M_{b1} causes much higher melt rates than M_{b2} close to the grounding line, where melt rates are always the highest.

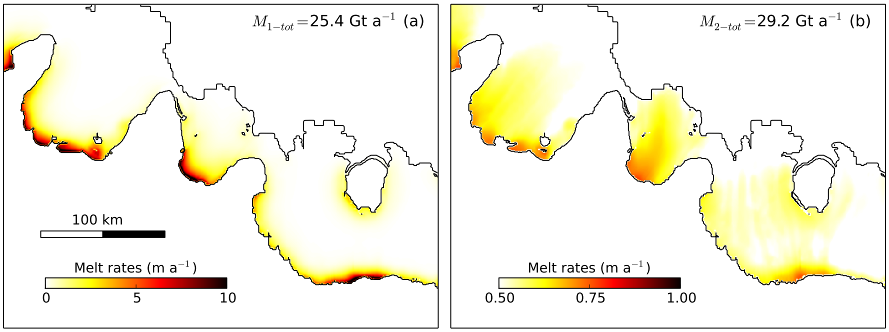

Figure 3. Initial fields of medium M_{b1} (a) and M_{b2} (b) sub-ice shelf melt rates for the B_e/S initialisation. The sum of melt rates over the computational domain, written at the top right of panels, is comparable to current values (Rignot et al., 2013; Depoorter et al., 2013, and M. Depoorter, personal communication, 2016; Supplementary Table).

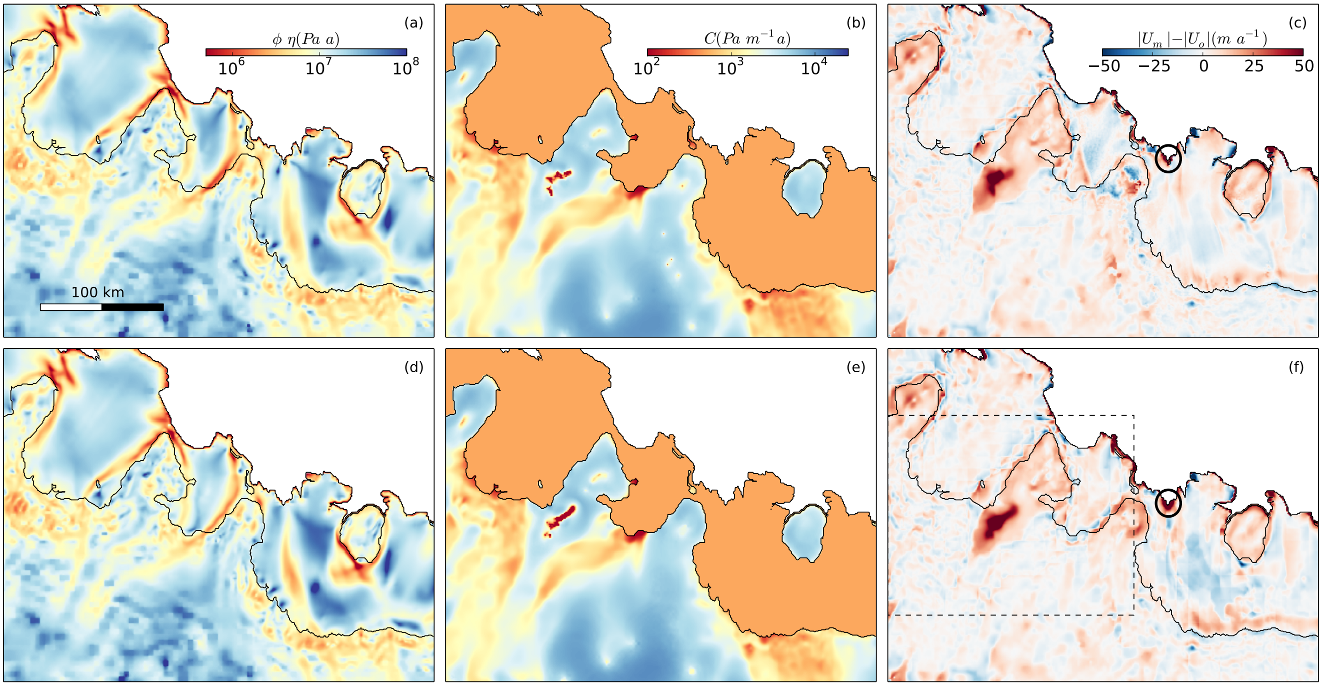

Figure 4. Results of the control method for B/S and B/U (a,b,c) and RF/S (d,e,f) initialisations, for linear sliding. Vertically averaged effective viscosity (a,d), basal friction coefficient (b,e) (for current ice shelves, the value of $C = 500\ Pa\ m^{-1}\ a$ is prescribed for transient simulations) and difference between modelled and observed velocities (c,f). The circles indicate PPw (c,f). The dashed box marks the large mismatch that are discussed in the text, and shown in more details in Supplementary Figure 1 (f).

3 Results

3.1 Data assimilation

The L-curve analysis performed by Berger et al. (2016) to optimise regularisation still holds for our extended domain and nonlinear sliding, even though it was originally applied to a smaller domain and linear sliding.

The root mean square error between modelled and observed velocities after data assimilation is $\approx$ 14 m a^{-1} for B_e/S and B_e/U initialisations, and $\approx$ 13 m a^{-1} for RF/S initialisation, and is independent of the applied sliding law. Such mismatches are similar to what was already computed by control methods applied to the Antarctic ice sheet (e.g. Fürst et al., 2015; Cornford et al., 2015). The largest mismatches ~~is~~are found at the calving front~~and at the~~, on ice rises and promontories~~. We also find a large mismatch~~, as well as upstream of the TB/HB promontory (Figure 4). We attribute ~~it~~the latter to the poor consistency between the high observed surface slope and thickness combined with low surface velocities (Supplementary Figure 1), as high driving stresses should induce high velocities. The control method cannot deal with such a non-physical combination for a steady-state ice sheet: it decreases the friction during the first iterations, and further attempts to catch up with the consequent mismatch through ice stiffening during the following iterations.

A significant difference between the two datasets appears in the vicinity of PPw (Figure 4), where the mismatch is lower when using the *high-resolution* dataset. There, omitting PPw in the control method leads to an excessive ice stiffening (Figure 5 in Berger et al., 2016).

The central parts of ice shelves are comparatively more viscous, except within rifting areas, where the viscosity can be few orders of magnitudes smaller. The friction coefficient is comparatively small beneath the ice streams of WRG, HB and TB, and few orders of magnitude higher where ice velocity is small, such as in between ice streams and beneath ice promontories and rises. We show these results in Figure 4 with linear sliding.

3.2 Initial speed up after unpinning

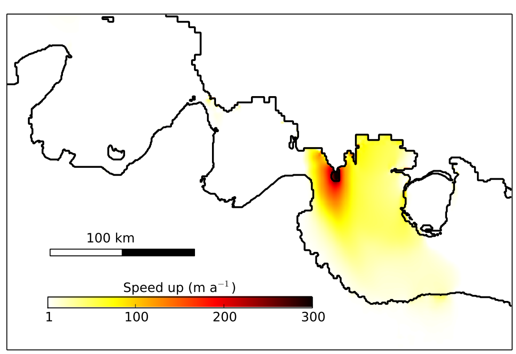

Figure 5. Speed up due to unpinning after 50 a for medium melt rates M_{b1} and linear sliding. ~~Velocity absolute~~Absolute velocity differences (m a^{-1}) between $B_e/U/L/M_{b1}/A_m$ and $B_u/U/L/M_{b1}/A_m$.

Unpinning (for B_e/U initialisation) induces an instantaneous acceleration of the WRG ice shelf by up to 300 m a^{-1} at the former location of PPw. After 50 a, the acceleration has propagated over almost the entire ice shelf up to the grounding line, but unpinning does not affect the nearby ice shelves of HB and East Ragnhild Glacier (Figure 5). The central flowline of the WRG ice stream migrates westward and relocates at an almost equal distance from the HB/WRG promontory and DIR within a few years. The velocities at the ice-shelf front are $\approx 20\%$ larger than for B_e/S initialisation. Overall, the comparatively faster ice shelf induces a less advanced grounding line at the end of simulations (about 10 km). The velocity increase near the HB/WRG promontory leads to thinning of its eastward side, making its saddle area afloat and turning it into an ice rise more rapidly than for B_e/S and RF/S initialisations.

3.3 Main steps of grounding-line migration

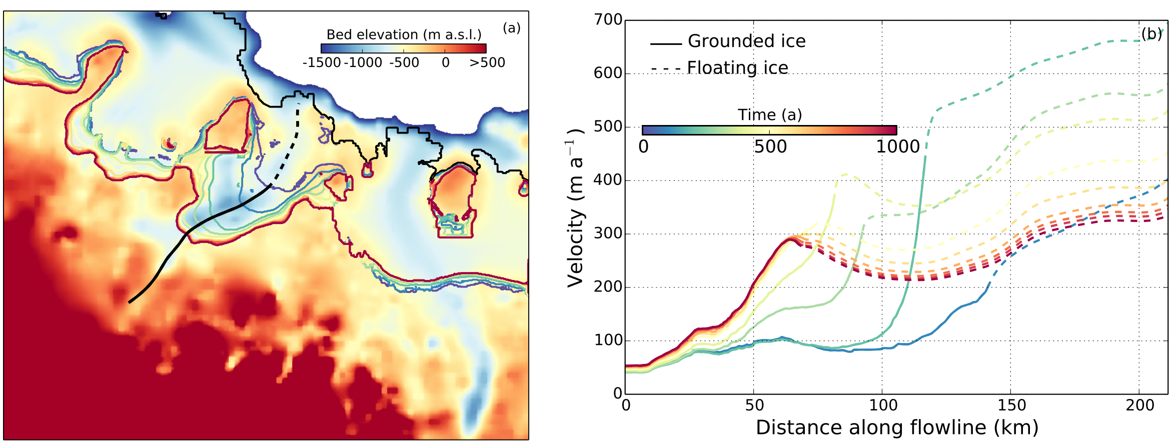

Figure 6. Grounding-line migration for the $B_e/S/L/M_{b1}/A_m$ experiment. (a) Bed elevation in the background, grounding lines are shown every 100 years (colorscale shown in (b)) and the dashed line shows the central flowline of HB. (b) Ice velocity profiles along the central flowline of HB, shown every 100 years. The grounding-line position is marked by the limit between solid and dashed parts of profiles.

The grounding line migrates similarly for medium melt-rates experiments with linear sliding (Figure 7) and nonlinear sliding. Here we present the common successive steps of all scenarios regarding grounding-line migration and ice dynamics (Figure 6 and Supplementary Movie).

The HB ice shelf/sheet system is by far the most dynamic of the three glaciers. During the first century, its grounding line retreats relatively slowly and the pinning points PPhs (Figure 1) detach from the ice-shelf base. The subsequent unpinning of PPhs is followed by an acceleration of the grounding-line retreat over the deepest part of the bed, along with a speed up of ice increasing from $\approx 20\%$ to 100% in a hundred year or so. During these rapid changes, two sudden jumps (the second being less dramatic than the first) in velocity and grounding-line retreat rates occur when the grounding line retreats over two consecutive troughs imprinting the bed. During the following years, the grounding line and velocities of HB stabilise progressively as the grounding line gets closer to the downsloping part of the bed. By the end of the simulations, the two saddles linking the TB/HB and HB/WRG promontories to the main ice sheet get successively afloat until the two promontories ~~collapse~~transition into ice rises, and the grounding line of HB has retreated by up to 100 km. The consequent loss of buttressing eventually produces a small retreat of the TB grounding line for the highest melt rates scenarios.

The B_e/U initialisation produces faster retreat of grounding lines than the B_e/S initialisation, which produces faster retreat than the RF/S initialisation. In particular, the saddle of the HB/WRG promontory gets afloat the most rapidly. The grounding lines of TB and WRG re-advance over up to tens of kilometres for low-melt scenarios.

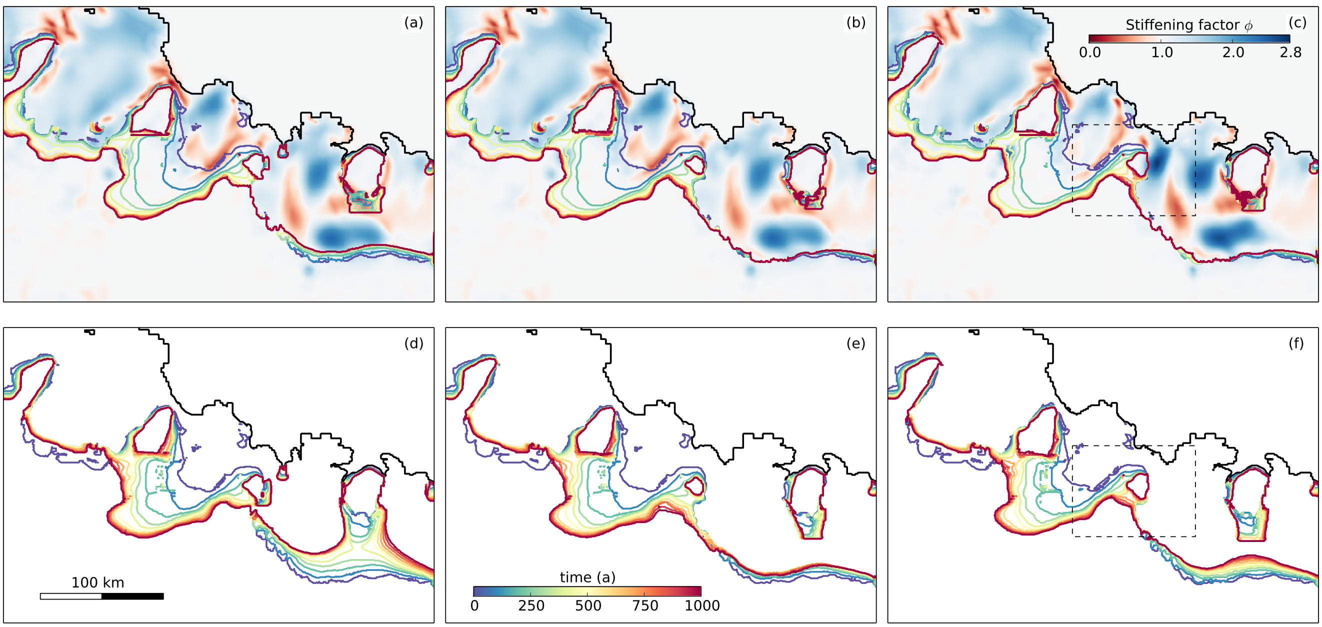

Figure 7. Grounding-line migration for medium melt rates and linear sliding. Melt rates M_{b1} (a,b,c) and M_{b2} (d,e,f). Experiments $B_e/S/L/M_{b1}/A_m$ (a), $B_e/U/L/M_{b1}/A_m$ (b), $RF/S/L/M_{b1}/A_m$ (c), $B_e/S/L/M_{b2}/A_m$ (d), $B_e/U/L/M_{b2}/A_m$ (e) and $RF/S/L/M_{b2}/A_m$ (f). Grounding lines are shown every 100 years. In (a,b,c) the stiffening factor field is shown in the background and a dashed line window is drawn to ~~show~~point out the area where excessive stiffening occurs when omitting PPw in data assimilation.

4 Discussion

Most of the continental shelf beneath the WAIS is ~~deeply depressed~~lower than sea level, making the ice sheet prone to ~~widespread~~undergo a MISI (Ritz et al., 2015; Mercer, 1978; Joughin and Alley, 2011). With respect to the ~~shelf depression~~bed topography, the EAIS ~~is potentially~~appears more stable, but its volume of ice is ten times larger than its western counterpart. It is therefore crucial to investigate a potential unstable retreat of grounding lines that may further affect the ice-sheet stability. Here, our simulations systematically show an unstable retreat of HB over the next few hundreds years regardless of the applied sub-ice shelf melt rates, sliding laws and initialisations (Figure 7 and Supplementary Movie). Half of the simulations also predict the retreat of the neighbouring glacier TB for melt rates comparable to current observations. ~~In total~~Overall, the contribution of the studied area to sea-level rise is ~~25 ± 10~~30 ± 10 mm for the next millennium, which needs to be put in perspective with the comparatively small domain (representing about 1% of the Antarctic ice sheet) and the possible nonlinear effects due to future oceanic forcing that are neglected in this study.

After a ~~few hundred years~~century, the HB grounding-line ~~is quickly retreating at~~retreat reaches its highest speed, 1 km a^{-1} ~~, and the ice-shelf velocities reach 700 m a^{-1}~~ for the $B_e/S/L/M_{b1}/A_m$ experiment and 500 m a^{-1} for the $B_e/S/L/M_{b2}/A_m$ experiment, further inducing after a couple of decades a peak in ice-shelf velocities, attaining 700 m a^{-1} for the latter two experiments when the grounding line retreats over the deepest part of the bed (Figure 6). The retreat is ~~only slightly modulated~~thus influenced by the type and amplitude of melt rates (Figure 8). ~~, indicating that it is mostly driven by a MISI~~We also evaluated the MISI part on the retreat of HB, by switching off the sub ice-shelf melting during the $B_e/S/L/M_{b1}/A_m$ when the grounding line retreats over the upsloping part of the bed, without altering the melt rates beneath the other ice shelves. The experiment, shown in Supplementary Figure 3, demonstrates that the grounding line retreat is substantially affected by a MISI, even though not entirely. However, none of the simulations show a retreat of the WRG grounding line, despite the presence of an incised valley of about 1200 m deep beneath the ice upstream of the grounding line (Figure 1). This valley is also narrow and starts tens of kilometres upstream of the current grounding line, while the depression beneath the HB grounded ice is wider and starts closer to the grounding line. This accords with the ideal simulations of Gudmundsson et al. (2012), who showed that a wider trough upstream of a grounding line reduces the buttressing exerted by the ice shelf, which enhances the grounding-line retreat rate.

During the ~~unstable~~ retreat of HB, the ice-shelf thickness is halved compared to ~~the~~ initial ~~thickness~~conditions. Meanwhile, the thickness of the WRG ice shelf remains almost constant in time near the east side of the HB/WRG promontory. The consequence is an increase of the ice flux coming from the promontory's saddle and going towards the HB ice shelf, reducing the width of the saddle from its western side and eventually making the HB/WRG promontory an ice rise when its saddle becomes afloat. The retreat of TB depends on the melt-rates type and amplitude. All the low amplitude and the M_{b2} medium amplitude melt rates lead to an advance of its grounding line, while the other scenarios lead to a retreat. However, this contrasting behaviour only slightly modulates the time span by which the saddle of the TB/HB promontory gets afloat, for which the substantial thinning of the HB ice shelf is the major driver.

~~Current~~The observed grounding lines fringed and buttressed by ice promontories (such as for HB) are ~~relatively~~currently stable in the studied area, even resting on upsloping bed (also shown by Gudmundsson et al., 2012, for synthetic numerical experiments). However, small amounts of sub-ice shelf melting clearly induce rapid grounding-line retreat and ~~collapse~~transition of the promontories into ice rises. ~~This unstable behaviour~~Such a quick transition is corroborated by Favier and Pattyn (2015), showing that promontories are transient features of grounding-line retreat, when they are characterized by an overdeepening upstream of the ~~pinning~~pinned area.

Most low and several medium melt rates scenarios lead to an advance of the WRG grounding line upstream of DIR (Figure 7), even though we excavated the area below the ice shelf. Because the bathymetry of ice-shelf cavities is poorly constrained, advancing grounding lines must be cautiously interpreted~~. However, the related~~, and this potentially spurious effect on sea level thus calls for a better knowledge of bathymetry beneath ice shelves.

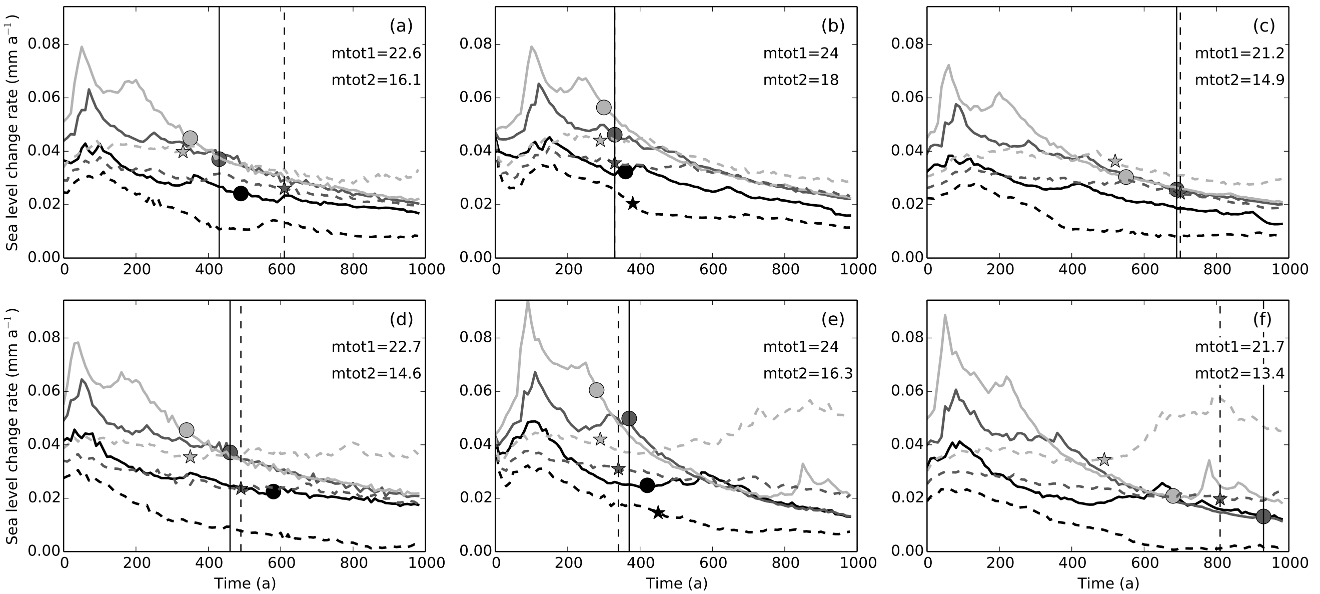

Figure 8. Contribution to sea level for all transient simulations. Linear sliding (a,b,c) and nonlinear sliding (d,e,f) experiments. Experiments using B_e/S (a,d), B_e/U (b,e) and RF/S (c,f) initialisations. Solid and dashed lines show M_{b1} and M_{b2} melt rates, respectively. The brighter the line, the higher the melt-rate amplitude. The circles (in M_{b1} lines) and triangles (in M_{b2} lines) markers indicate the time by which the HB/WRG promontory ~~turns~~transitions into an ice rise, which is also marked by a vertical line (solid or dashed) for the medium melt rates experiments. The two numbers shown at the top right of each panel indicate the contribution to sea-level change in mm after 500 a of medium melt rates experiments (mtot1 for M_{b1}, and mtot2 for M_{b1}).

Unpinning of the WRG ice shelf mildly affects the global contribution to sea level, ~~which is rather similar to the experiments using~~increasing it by 10% compared to the B_e/S initialisations (Figure 8). However, the decrease of buttressing stemming from unpinning thins the WRG ice shelf and accelerates the retreat of the HB/WRG promontory's saddle from its eastern side: the saddle gets afloat ~~a few hundred years~~two centuries earlier (Figure 8). ~~Such a large difference in timing compared to the differences in sea-level contribution~~This indicates a large sensitivity of promontories deglaciation to a loss of buttressing, similarly to the unstable retreat pointed out in Favier and Pattyn (2015). The loss of buttressing induced by unpinning also cancels the advance of the WRG grounding line simulated by the experiments using B_e/S initialisations (Figure 7b), but does not have enough effect to induce an unstable retreat over the upsloping bed area upstream of the grounding line. On the west side of the HB/WRG promontory, unpinning of PPhs occurring after ~~about~~less than 100 years of simulation precedes by few years the acceleration of the ongoing ~~unstable~~ retreat of the HB grounding line (Supplementary Movie). However, quantifying the contribution of PPhs unpinning to the grounding-line retreat is not straightforward, since unpinning is effective when the HB grounding line retreats over the deepest, hence with the largest potential for inducing a MISI.

Besides the MISI-driven consequences on sea level, sub-ice shelf melting is the other main driver of the retreat. Different behaviours emerge from the two types of melt-rate parametrisations. During the first few hundreds of years, sea-level contribution is more or less a linear function of melt-rates amplitude. The form of M_{b1} induces high melt rates at the grounding line when it retreats over the deep trough beneath HB. The contribution to sea level is then a function of pure melting and dynamic thinning, inducing peaks of sea-level contribution after about ~~150 a~~a century. In the case of M_{b2} melt rates, this peak is replaced by a milder bump in sea-level contribution (Figure 7) since the pure-melting contribution is lower. After 500 a, the retreat of the HB grounding line is less rapid and the contribution to sea level is then mostly due to melting, and to a lesser extent due to dynamic thinning. Since the M_{b1} melt rates induce more melting at large depth and almost no melting closer to the surface compared to the M_{b2} of similar amplitudes, the M_{b1} melt rates become lower compared to the M_{b2} melt rates, except for the lowest melt rates where this is the opposite. After $\approx$ 800 a, a sudden increase in sea-level contribution occurs for nonlinear sliding and the high M_{b2} melt rates (Figure 8(e,f)), which is due to ungrounding of the promontory saddle between the Lazarev ice shelf and the Unnamed Glacier (Figure 1). This peculiar behaviour that does not occur for the other experiments is the reason why we indicate the sea-level contribution after 500 a (Figure 8.

Compared to linear sliding, nonlinear sliding (with $m = 1/3$) should enhance basal sliding when ice velocity increases. The acceleration of HB during its ~~unstable~~ retreat consequently yields higher velocities and faster retreat rates of the grounding line for the nonlinear case, hence leading to a higher contribution to sea level from HB~~(Figure 8)~~. At the scale of the domain, this is however difficult to grasp the differences between the two sliding laws, since they induce similar contributions after 500 a.

As already shown by Berger et al. (2016), omitting the pinning point PPw in data assimilation induces erroneous ice stiffening nearby. Initialising transient simulations with such stiffening leads to a spurious decrease in sea-level contribution by 10% compared to the experiments using B_e/S initialisation. The transient evolution of the WRG grounding line looks similar to the unpinning experiments, pointing out the spatially limited effects of the excessively stiffened ice. However, the stiffening effect largely alters the timing of deglaciation of the HB/WRG promontory (Figure 8) and delays it by approximately 500 a. Moreover, any further local change in the boundary condition between the pinning points and the ice shelf, including the extreme - but possible - event of unpinning (for instance induced by a substantial thinning of ice shelves; see Paolo et al., 2015) cannot be simulated by the model if the pinning point is omitted in the first place.

Since the early 2000s, uncertainties of ice-sheet modelling outputs have been reduced by substantial numerical improvements, enabling to grasp more accurately key processes such as grounding-line migration (Pattyn and Durand, 2013). This improvement was also made possible by the increasing computational power. We are now able to simulate the behaviour of the WAIS using higher order models at a high spatial resolution in the relevant areas for a wide range of scenarios over the next centuries (Cornford et al., 2015), which was not feasible a few years ago. Nevertheless, the lack of knowledge of essential parameters still affects simulations of the Antarctic ice sheet behaviour, hence preventing further decrease of uncertainties in sea-level predictions. Sub-ice shelf melting is a major driver of ice-sheet retreat and sea-level contribution (Figure 8). Even though forcing the ice sheet with parametrised melt rates (such as in this study) gives qualitative and informative insights on future sea-level contribution, the lack of knowledge of the cavity beneath ice shelves prevents the use of more advanced assessment based on ocean modelling (such as in Hattermann et al., 2014; De Rydt and Gudmundsson, 2016). Moreover, the ill-constrained shape of the ice-shelf cavity dictates how and if the grounding line advances, which also biases future sea-level predictions. Here, we demonstrates that sea-level predictions and timing of deglaciation can be substantially affected by ~~the type of sliding law,~~ a too shallow bathymetry and the absence of small pinning points, which all affect ice-sheet initialisation. Also, the exact representation of pinning points (ice rumples, rises and promontories) in the observational datasets, even if they are small, is key for more accurate predictions of future sea-level change and timing of ice-sheet retreat. Therefore, improving these predictions by the use of ice-sheet modelling relies on future improvements of our knowledge of the bathymetry beneath ice shelves and (small) pinning points.

5 Conclusions

We use the ice-sheet model BISICLES to evaluate the contribution of the outlet glaciers between the Lazarev and Roi Baudouin ice shelves in East Antarctica to future sea-level rise, with two different input datasets including or excluding an observed small pinning point (PPw) at the calving front. We also investigate the influence of various sub ice-shelf melt rates parametrisation and two types of Weertman-like sliding law (linear and nonlinear). Our results ~~show the likely future unstable retreat of the outlet glacier Hansenbreen (HB) within the next 150 a, which is~~suggest an unstable retreat of the Hansenbreen (HB) glacier within the next century. This retreat is equally driven by sub ice-shelf melting and marine ice sheet instability (MISI), while the other outlet glaciers are relatively stable over the next millennium. Where the ~~ice sheet is stable~~bed is downsloping towards the sea (no potential for a MISI), sub-ice shelf melting ~~strongly~~exclusively controls sea-level contribution. ~~Nonlinear sliding increases the sea-level contribution by 20% but does not affect the timing of deglaciation compared to linear sliding.~~ ~~Surprisingly, u~~Unpinning ~~(removing~~of PPw ~~after ice-sheet initialisation)~~ ~~hardly impacts the~~increases the sea-level contribution by 10%~~.~~ ~~However, it~~but substantially affects the timing of ice-sheet retreat in the most sensitive parts, such as the HB/WRG promontory which ~~collapses~~transition into an ice rise 200 a in advance. On the other hand, omitting PPw during the initialisation of the ice sheet yields local excessive ice-shelf stiffening, which decreases the sea-level contribution by 10% and delays the HB/WRG promontory ~~collapse~~transition by 500 a in transient simulations. Even small ~~P~~pinning points should be accounted for in ice-sheet modelling because they affect transient ice-dynamical behaviour and grounding-line retreat~~ when not accounted for properly~~. This study calls for a better knowledge of Antarctic ice sheet margins, including the bathymetry beneath ice shelves and the characteristics - ice velocity and ice/bed geometry - of even the smallest pinning points, in order to ~~reduce uncertainties in sea-level predictions~~improve our ability to predict future Antarctic ice sheet margins.

Acknowledgements. This paper forms a contribution to the Belgian Research Programme on the Antarctic (Belgian Federal Science Policy Office), Project SD/CA/06A (Constraining Ice Mass Change in Antarctica, IceCon). R. Drews was partially supported by the Deutsche Forschungsgemeinschaft (DFG) in the framework of the priority programme "Antarctic Research with comparative investigations in Arctic ice areas" by the grant MA 3347/10-1. BISICLES development is led by D.F. Martin at Lawrence Berkeley National Laboratory, California, USA, and S.L. Cornford at the University of Bristol, UK, with financial support provided by the U.S. Department of Energy and the UK Natural Environment Research Council. Simulations were carried out using the computational facilities of the HPC computing center at Université libre de Bruxelles. We are grateful to M. Depoorter for providing us with current sub-ice shelf melt rates.

References

Arthern, R. J., Hindmarsh, R. C. a., and Williams, C. R. (2015). Flow speed within the Antarctic ice sheet and its controls inferred from satellite observations. Journal of Geophysical Research: Earth Surface, pages n/a–n/a.

Arthern, R. J., Winebrenner, D. P., and Vaughan, D. G. (2006). Antarctic snow accumulation mapped using polarization of 4.3-cm wavelength microwave emission. Journal of Geophysical Research, 111(D6):D06107.

Beckmann, a. and Goosse, H. (2003). A parameterization of ice shelf-ocean interaction for climate models. Ocean Modelling, 5(2):157–170.

Berger, S., Favier, L., Drews, R., Derwael, J.-J., and Pattyn, F. (2016). The control of an uncharted pinning point on the flow of an Antarctic ice shelf. Journal of Glaciology, 62(231):37–45.

Borstad, C. P., Rignot, E., Mouginot, J., and Schodlok, M. P. (2013). Creep deformation and buttressing capacity of damaged ice shelves: theory and application to Larsen C ice shelf. The Cryosphere, 7(6):1931–1947.

Callens, D., Matsuoka, K., Steinhage, D., Smith, B., Witrant, E., and Pattyn, F. (2014). Transition of flow regime along a marine-terminating outlet glacier in East Antarctica. The Cryosphere, 8(3):867–875.

Callens, D., Thonnard, N., Lenaerts, J. T., Van Wessem, J. M., Van De Berg, W. J., Matsuoka, K., and Pattyn, F. (2015). Mass balance of the Sør Rondane glacial system, East Antarctica. Annals of Glaciology, 56(70):63–69.

Cornford, S. L., Martin, D. F., Payne, a. J., Ng, E. G., Le Brocq, a. M., Gladstone, R. M., Edwards, T. L., Shannon, S. R., Agosta, C., van den Broeke, M. R., Hellmer, H. H., Krinner, G., Ligtenberg, S. R. M., Timmermann, R., and Vaughan, D. G. (2015). Century-scale simulations of the response of the West Antarctic Ice Sheet to a warming climate. The Cryosphere, 9(2):1887–1942.

De Rydt, J. and Gudmundsson, G. H. (2016). Coupled ice shelf-ocean modeling and complex grounding line retreat from a seabed ridge. Journal of Geophysical Research: Earth Surface, (March).

Deconto, R. M. and Pollard, D. (2016). Contribution of Antarctica to past and future sea-level rise. Nature, 531(7596):591–597.

Depoorter, M. a., Bamber, J. L., Griggs, J. a., Lenaerts, J. T. M., Ligtenberg, S. R. M., van den Broeke, M. R., and Moholdt, G. (2013). Calving fluxes and basal melt rates of Antarctic ice shelves. Nature, 502(7469):89–92.

Drews, R. (2015). Evolution of ice-shelf channels in Antarctic ice shelves. The Cryosphere, 9(3):1169–1181.

Durand, G., Gagliardini, O., de Fleurian, B., Zwinger, T., and Le Meur, E. (2009). Marine ice sheet dynamics: Hysteresis and neutral equilibrium. Journal of Geophysical Research: Earth Surface, 114(F3):F03009.

Favier, L., Gagliardini, O., Durand, G., and Zwinger, T. (2012). A three-dimensional full Stokes model of the grounding line dynamics: Effect of a pinning point beneath the ice shelf. The Cryosphere, 6(1):101–112.

Favier, L. and Pattyn, F. (2015). Antarctic ice rise formation , evolution , and stability. Geophysical Research Letters, 42(11):2015GL064195.

Fretwell, P., Pritchard, H. D., Vaughan, D. G., Bamber, J. L., Barrand, N. E., Bell, R., Bianchi, C., Bingham, R. G., Blankenship, D. D., Casassa, G., Catania, G., Callens, D., Conway, H., Cook, a. J., Corr, H. F. J., Damaske, D., Damm, V., Ferraccioli, F., Forsberg, R., Fujita, S., Gim, Y., Gogineni, P., Griggs, J. a., Hindmarsh, R. C. a., Holmlund, P., Holt, J. W., Jacobel, R. W., Jenkins, A., Jokat, W., Jordan, T., King, E. C., Kohler, J., Krabill, W., Riger-Kusk, M., Langley, K. a., Leitchenkov, G., Leuschen, C., Luyendyk, B. P., Matsuoka, K., Mouginot, J., Nitsche, F. O., Nogi, Y., Nost, O. a., Popov, S. V., Rignot, E., Rippin, D. M., Rivera, A., Roberts, J., Ross, N., Siegert, M. J., Smith, a. M., Steinhage, D., Studinger, M., Sun, B., Tinto, B. K., Welch, B. C., Wilson, D., Young, D. a., Xiangbin, C., and Zirizzotti, A. (2013). Bedmap2: Improved ice bed, surface and thickness datasets for Antarctica. Cryosphere, 7(1):375–393.

Fürst, J. J., Durand, G., Gillet-Chaulet, F., Merino, N., Tavard, L., Mouginot, J., Gourmelen, N., and Gagliardini, O. (2015). Assimilation of Antarctic velocity observations provides evidence for uncharted pinning points. The Cryosphere, 9(2):1461–1502.

Fürst, J. J., Durand, G., Gillet-chaulet, F., Tavard, L., Rankl, M., Braun, M., and Gagliardini, O. (2016). The safety band of Antarctic ice shelves. Nature Clim. Change, 6:2014–2017.

Goldberg, D., Holland, D. M., and Schoof, C. (2009). Grounding line movement and ice shelf buttressing in marine ice sheets. Journal of Geophysical Research: Earth Surface, 114(F4):F04026.

Gong, Y., Cornford, S. L., and Payne, A. J. (2014). Modelling the response of the Lambert Glacier–Amery Ice Shelf system, East Antarctica, to uncertain climate forcing over the 21st and 22nd centuries. The Cryosphere, 8(3):1057–1068.

Gudmundsson, G. H., Krug, J., Durand, G., Favier, L., and Gagliardini, O. (2012). The stability of grounding lines on retrograde slopes. Cryosphere, 6(6):1497–1505.

Hattermann, T., Smedsrud, L. H., Nøst, O. A., Lilly, J. M., and Galton-Fenzi, B. K. (2014). Eddy-resolving simulations of the Fimbul Ice Shelf cavity circulation: Basal melting and exchange with open ocean. Ocean Modelling, 82(October):28–44.

Humbert, a. and Steinhage, D. (2011). The evolution of the western rift area of the Fimbul Ice Shelf, Antarctica. Cryosphere, 5(4):931–944.

Jay-Allemand, M., Gillet-Chaulet, F., Gagliardini, O., and Nodet, M. (2011). Investigating changes in basal conditions of Variegated Glacier prior to and during its 1982-1983 surge. Cryosphere, 5(2005):659–672.

Joughin, I. and Alley, R. B. (2011). Stability of the West Antarctic ice sheet in a warming world. Nature Geoscience, 4(8):506–513.

Le Brocq, A. M., Payne, A. J., and Vieli, A. (2010). An improved Antarctic dataset for high resolution numerical ice sheet models (ALBMAPv1). Earth System Science Data, 2(2007):247–260.

Livingstone, S. J., Ó Cofaigh, C., Stokes, C. R., Hillenbrand, C.-D., Vieli, A., and Jamieson, S. S. (2012). Antarctic palaeo-ice streams. Earth-Science Reviews, 111(1-2):90–128.

MacAyeal, D. R. (1993). A tutorial on the use of control methods in ice-sheet modeling. Journal of Glaciology, 39(131):91–98.

Matsuoka, K., Hindmarsh, R. C., Moholdt, G., Bentley, M. J., Pritchard, H. D., Brown, J., Conway, H., Drews, R., Durand, G., Goldberg, D., Hattermann, T., Kingslake, J., Lenaerts, J. T., Martín, C., Mulvaney, R., Nicholls, K., Pattyn, F., Ross, N., Scambos, T., and Whitehouse, P. L. (2015). Antarctic ice rises and rumples: their properties and significance for ice-sheet dynamics and evolution. Earth-Science Reviews, 150(November):724–745.

Mercer, J. (1978). West Antarctic ice sheet and CO2 greenhouse effect: a threat of disaster. Nature, 271.

Morlighem, M., Seroussi, H., Larour, E., and Rignot, E. (2013). Inversion of basal friction in Antarctica using exact and incomplete adjoints of a higher-order model. Journal of Geophysical Research: Earth Surface, 118(3):1746–1753.

Mouginot, M., Rignot, E., Gim, Y., Kirchner, D., and Lemeur, E. (2014). Low-frequency radar sounding of ice in East Antarctica and southern Greenland. Annals of Glaciology, 55(67):138–146.

Paolo, F. S., Fricker, H. A., and Padman, L. (2015). Volume loss from Antarctic ice shelves is accelerating. Science, 348(6232):327–332.

Pattyn, F. (2010). Antarctic subglacial conditions inferred from a hybrid ice sheet/ice stream model. Earth and Planetary Science Letters, 295(3-4):451–461.

Pattyn, F. and Durand, G. (2013). Why marine ice sheet model predictions may diverge in estimating future sea level rise. Geophysical Research Letters, 40(16):4316–4320.

Pritchard, H. D., Ligtenberg, S. R. M., Fricker, H. a., Vaughan, D. G., van den Broeke, M. R., and Padman, L. (2012). Antarctic ice-sheet loss driven by basal melting of ice shelves. Nature, 484(7395):502–505.

Raymond, C. F. (1983). Deformation in the vicinity of ice divides. Journal of Glaciology, 29(103):357–373.

Rignot, E., Jacobs, S., Mouginot, J., and Scheuchl, B. (2013). Ice-Shelf Melting Around Antarctica. Science, 341(6143):266–270.

Rignot, E., Velicogna, I., Van Den Broeke, M. R., Monaghan, A., and Lenaerts, J. (2011). Acceleration of the contribution of the Greenland and Antarctic ice sheets to sea level rise. Geophysical Research Letters, 38(5):1–5.

Ritz, C., Edwards, T. L., Durand, G., Payne, A. J., Peyaud, V., and Hindmarsh, R. C. A. (2015). Potential sea-level rise from Antarctic ice-sheet instability constrained by observations. Nature, 528:115–118.

Schmeltz, M., Rignot, E., and MacAyeal, D. R. (2001). Ephemeral grounding as a signal of ice-shelf change. Journal of Glaciology, 47(156):71–77.

Schmidtko, S., Heywood, K. J., Thompson, A. F., and Aoki, S. (2014). Multidecadal warming of Antarctic waters. Science, 346(6214):1227–1231.

Schoof, C. (2007). Ice sheet grounding line dynamics: Steady states, stability, and hysteresis. Journal of Geophysical Research: Earth Surface, 112(F3):F03S28.

Thomas, R. H. and Bentley, C. R. (1978). A model for Holocene retreat of the West Antarctic Ice Sheet. Quaternary Research, 10(2):150–170.

Tinto, K. J. and Bell, R. E. (2011). Progressive unpinning of Thwaites Glacier from newly identified offshore ridge: Constraints from aerogravity. Geophysical Research Letters, 38(20):L20503.

Weertman, J. (1957). On the sliding of glaciers. Journal of Glaciology, 3:33–38.

Weertman, J. (1974). Stability of the junction of an ice sheet and an ice shelf. Journal of Glaciology, 13(67):3–11.